Integrated high pressure microhydraulic actuation and control for surgical instruments

A. J. M. Moers · M. F. L. De Volder · D. Reynaerts

Abstract To reduce the surgical trauma to the patient, minimally invasive surgery is gaining considerable importance since the eighties. More recently, robot assisted minimally invasive surgery was introduced to enhance the surgeon's performance in these procedures. This resulted in an intensive research on the design, fabrication and control of surgical robots over the last decades. A new development in the field of surgical tool manipulators is presented in this article: a flexible manipulator with distributed degrees of freedom powered by microhydraulic actuators. The tool consists of successive flexible segments, each with two bending degrees of freedom. To actuate these compliant segments, dedicated fluidic actuators are incorporated, together with compact hydraulic valves which control the actuator motion. Especially the development of microvalves for this application was challenging, and are the main focus of this paper. The valves distribute the hydraulic power from one common high pressure supply to a series of artificial muscle actuators. Tests show that the angular stroke of the each segment of this medical instrument is 90°.

Keywords Surgical manipulator · Minimally invasive surgery · High pressure microvalves · Hydraulic microactuator

1 Introduction

In minimally invasive surgery (MIS), natural orifice transluminal endoscopic surgery (NOTES), and robot assisted

A. J. M. Moers · M. F. L. De Volder (✉) · D. Reynaerts
Department of Mechanical Engineering, K.U.Leuven,
Celetijnenlaan 300B,
3001, Leuven, Belgium
e-mail: michael.devolder@mech.kuleuven.be

surgery, access to the patient's body is provided via small incisions in the skin and the tissue below (Ballantyne 2002). To reduce the trauma caused by the intervention, the diameter of the surgical instrument should be as small as possible. An important issue is however the manoeuvrability of these tools once they are inserted into the body of the patient. To improve minimally invasive surgery further research on the mechanical design of highly-dextrous surgical manipulators is therefore required (Ballantyne 2002).

An explicit problem regarding the manoeuvrability, is that the positioning of the surgical tools is restricted by the access point (trocar) defined by the incision, and to solve this issue, local actuation, e.g. by a modular concept (Harada et al. 2010) is required. Many of the currently used systems rely on cables to transmit the power from external actuators or the fingers of the surgeon to the manipulators at the tip of the surgical instruments (Tadano and Kawashima 2010). While cable systems are reliable and low cost, the number of degrees of freedom that can be actuated via a cable transmission is limited. Furthermore they often suffer from stick–slip or backlash and have a limited life-time (Nayyar and Gupta 2010). Therefore an actuation method which is powerful and compact is preferably integrated in the manipulator (Reynaerts et al. 1998; Takemura et al. 2008; Jeong and Konishi 2006; Ruzzu et al. 1998).

Especially for a surgical system which navigates far from the insertion point as shown schematically in Fig. 1, a high number of locally actuated degrees of freedom is required. As sketched in this figure, this research aims at developing manipulators which can be controlled over their full length, comparable to a snake. Such manipulators would enable positioning of the surgical instruments within a larger volume and around obstacles like organs without repositioning the tools through new access points. To accomplish this, a modular flexible hydraulic actuator design has been investigated. Snake-like robotic systems have received considerable

Fig. 1 Robotic assisted surgery with intra-corporal actuation. Top: Overview of the patient and the overall robotic system. Middle: Example of a surgical tool with multiple flexible active segments. Bottom: One tool segment powered by three hydraulic valves and antagonistic artificial muscle actuators
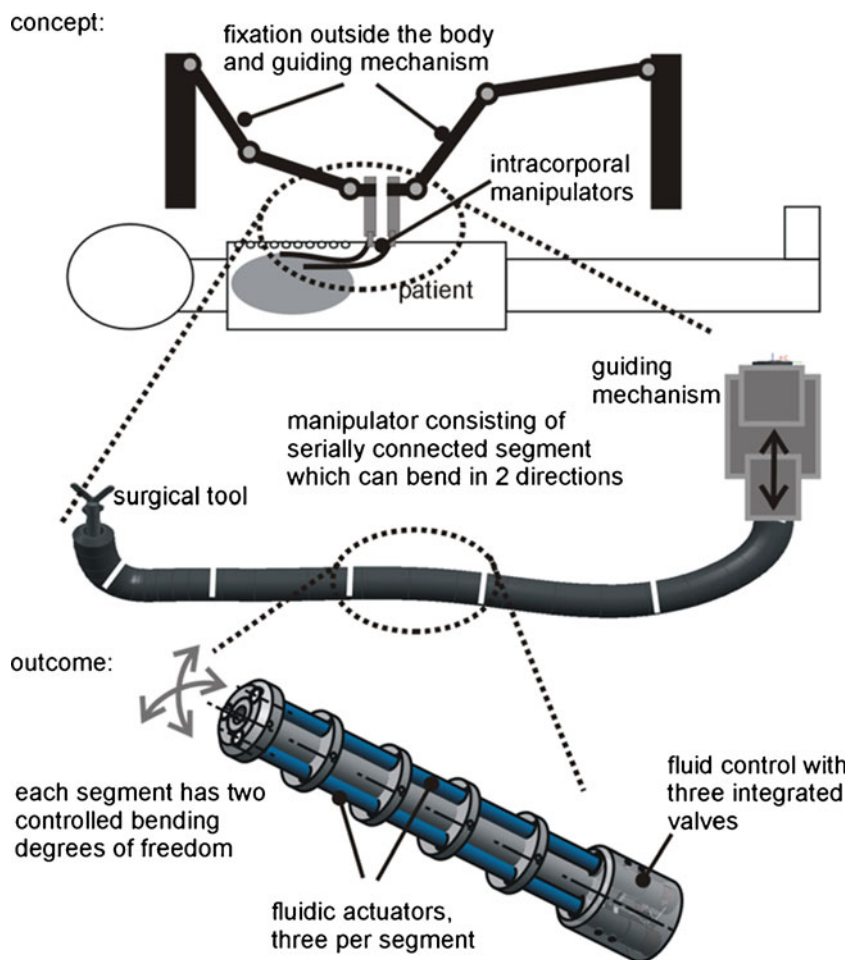
attention in the field of robotic research over the last years (Hirose et al. 1991; Webster et al. 2006; Kim et al. 2009; Konishi et al. 2001; Lu and Kim 2006; Konishi 2011; Watanabe et al. 2007b; Wakimoto et al. 2011; De Greef et al. 2009; Suzumori et al. 1996) The proposed system has been specifically developed for medical applications which, as will be clear from the specifications, required a high output force to navigate through and interact with the human body tissue. An important aspect of this research is the integrated control of the fluid pressure to the actuators. Therefore integrated compact hydraulic valves have been developed.

2 Objectives and specifications

In Table 1, the objectives for the envisaged manipulator are presented and related to the specifications of comparable systems (Peirs et al. 2004; Karimyan et al. 2009). The first column shows the specifications of current systems which are taken as a reference. The objectives of the proof of concept developed during this work are shown in the second column. The final objectives of a surgical device are represented in the third column.

The specified output force of 2 N is the force which is required for suturing of tissue as discussed by Peirs et al. (Peirs et al. 2004). The maximal diameter originates from the maximal diameter for NOTES (natural orifice transluminal surgery) (Karimyan et al. 2009). For the manoeuvrability, a surgical instrument that is handled by the hand of a surgeon is the reference which should ideally be achieved. The number of degrees of freedom in this case is six. The bandwidth of the system would ideally be about 10 Hz.

3 Manipulator layout

As shown in Fig. 1, the manipulator basically consists of active segments that are connected in series. In Fig. 2, one segment is represented. A single segment as depicted in Fig. 2 can bend in two degrees of freedom, and the final device consists of a series connection of these modules. The deformation of each segment determines the relative position of the surgical device with respect to the extra-corporal fixation of the system. Three actuators are placed in parallel around a flexible elastic tube that acts as a central bi-

	Specifications from current devices	Objectives	
		Proof of concept	Surgical device
Output force	2 N	1 N	2 N
Manooeuvrability	six DOF	±90° stroke per segment in two directions	six DOF without external instrument repositioning
Modularity	two modules	one module	at least five modules
Diameter	15 mm (NOTES)	15 mm	10 mm
Reliability	no failure	robust concept	no failure

Table 1 Specifications and objectives for the prototype

directional leaf spring providing also the neutral position of the device. This actuated device acts as a tool guiding channel for a surgical tool which can be inserted, retracted and rotated through the central channel. The system is in that sense comparable to current colonoscopes (Waye et al. 2009) but the novelty lies in the intra-corporal actuation.

The actuators of the system are incorporated in a mechanical base structure consisting of the elastic tube and spacer disks. It provides rigidity in the directions that are not actuated and has a low stiffness in the actuated directions. The remaining space between the actuators is used for both the hydraulic and electric power supply. At the end of the base structure of each segment, a hydraulic unit is placed to control the pressure delivered to the actuators. Throughout the manipulator, the centre is hollow, hereby providing a channel to guide the actual surgical tools such as a gripper, scissor or biopsy tips. Besides enabling translation and rotation of these tool, this concept also allows changing the tool or the tooltip during the surgical procedure. Rapid exchange of tools has been identified as a major factor in MIS procedures and a concept of a 'snake' with a fixed tool tip could not provide this.
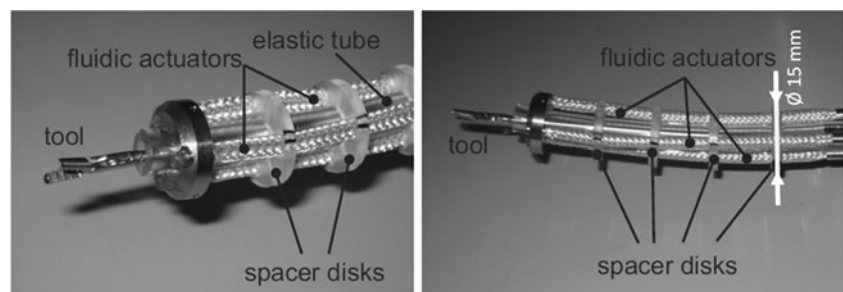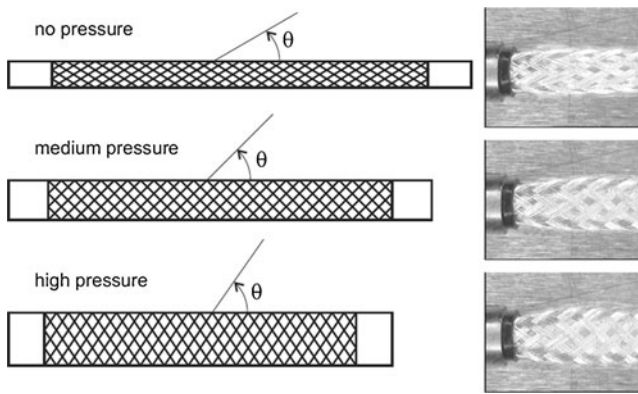
4 Fluidic actuators

As shown in Table 1, the tool needs to develop high forces in a restricted volume. Recent studies on hydraulic and pneumatic actuators revealed that these systems are particularly interesting for the development of extremely high force and power densities (i.e. the power per volume) at the microscale (De Volder and Reynaerts 2010; Gorissen et al. 2011; De Volder and Reynaerts 2009; De Volder et al. 2008; Yamaguchi et al. 2011; Watanabe et al. 2007a; Raoufi et al. 2008; De Volder et al. 2009). Furthermore these systems have shown to achieve high positioning accuracy (De Volder et al. 2008; De Volder et al. 2011; Stoianovici et al. 2007). Classic piston-cylinder actuators are relatively stiff, and therefore not preferable for this application, and therefore, research focussed on a particular type of high force elastic actuators . In literature, different names are used for this type of actuators: braided pneumatic muscles (Doumit et al. 2009; Caldwell et al. 1993), fluid actuated motor system (Gaylord 1958) McKibben artificial muscle actuators (Klute and Hannaford 2000) or McKibben actuator (De Volder et al. 2011). In literature, these actuators are often used in large robotic systems, using air as driving fluid to minimize weight. In this research, weight is not an issue given the small size of our system, and therefore, water is used in our experiments. Eventually, in a final medical application, physiological water will be the fluid to drive the segments.

Figure 3 shows the working principle of the McKibben actuator schematically. More details are discussed in (De Volder et al. 2011). The actuator consists of an elastic tube which is surrounded by a braided structure. Upon pressurisation, the inside the elastic tube will increase its diameter. The surrounding braided structure however constraints the radial expansion and as the angle of the braided mesh, couples the radial expansion to a lengthwise contraction of

Fig. 2 One segment consisting of three fluidic actuators, spacer disks and an elastic tube. The elastic acts as a tool channel for a grasping tool

Fig. 3 Working principle of the fluidic actuator showing the change in diameter and length of the actuator as it is pressurized

the actuator (see Fig. 3). If the actuator ends are fixed, the actuator will generate a counteracting force.

In the patent filed by Gaylord (Gaylord 1958), on this type of actuators, a basic equation to estimate the output force is presented. This research only requires an estimation of the force that allows to scale the dimensions of the actuators according to the system requirements. This model therefore assumes no friction losses, zero elasticity of the inner tubes and no wall thickness of the inner tubes.

$$F_{act} = p \frac{\pi d_{45°}^2}{2} \left(3\cos^2\theta - 1\right)$$

F_{act} is the output force, $d_{45°}$ is the diameter of the braided structure for $\theta = 45°$ and θ is the angle between each effective strand of the braided structure and a line drawn upon the surface of the structure parallel to its longitudinal axis (see Fig. 3). In the extended position, $\cos\theta$ seldom exceeds 0.9 ($\theta = 26°$) for a braided structure that contains sufficient strands to support the inner elastic tube. If the support of the elastic tubes is insufficient and the braided outer structure is too open, the elastic structure is not supported and cannot resist the applied pressure mechanical stress. The output force in the extended position is $0.7p\,\pi d_{45°}^2$. When $\theta = 45°$ pressure. In that case, the output force is $0.25p\,\pi d_{45°}^2$ which equals to the output force of a piston with the same diameter as a McKibben actuator. However, as θ increases, the output force of a McKibben actuator can be up to three times higher than that of a piston actuator with the same diameter. More details on both the fabrication and simulation of our McKibben actuators was presented in a former publication (De Volder et al. 2011).

Below the most interesting properties of these actuators are listed:

> *Flexible.* The actuator has a low bending stiffness. This is interesting especially when the actuators need to be

incorporated in a flexible manipulator that bends over its full range. Compared to hydraulic actuators with a piston, there are also no alignment issues. Only the end connections, the flexible inner tube and the outer braided sleeve need to be aligned during assembly.

High force density. At a supply pressure of 10 bar, the measured force output of an actuator with a diameter of 1.5 mm is 6 N. The resulting force per actuator cross section is 3.4 N/mm^2. A conventional hydraulic actuator with a piston supplied at 10 bar has an output force of only 1 N/mm^2 (De Volder and Reynaerts 2010; De Volder et al. 2011) (see theoretical analysis above).

Small size. It is possible to miniaturise the actuator down to a diameter of 1.5 mm which is important for the design of a manipulator of which the diameter is constrained (De Volder et al. 2011).

For the manipulator developed here, a specific McKibben actuator with a (non-inflated) diameter of 2.6 mm has been developed. In Fig. 4, the components of the end connections are presented. The inner connection (see Fig. 4(a)) is clamped at the inside of the silicone rubber tube. At the outside a connection tube is placed. During the assembly process, two component epoxy glue is applied on the end of the braided sleeve before the connecting tube is positioned. The braided sleeves used in this research are the shielding sleeves in coaxial cables.
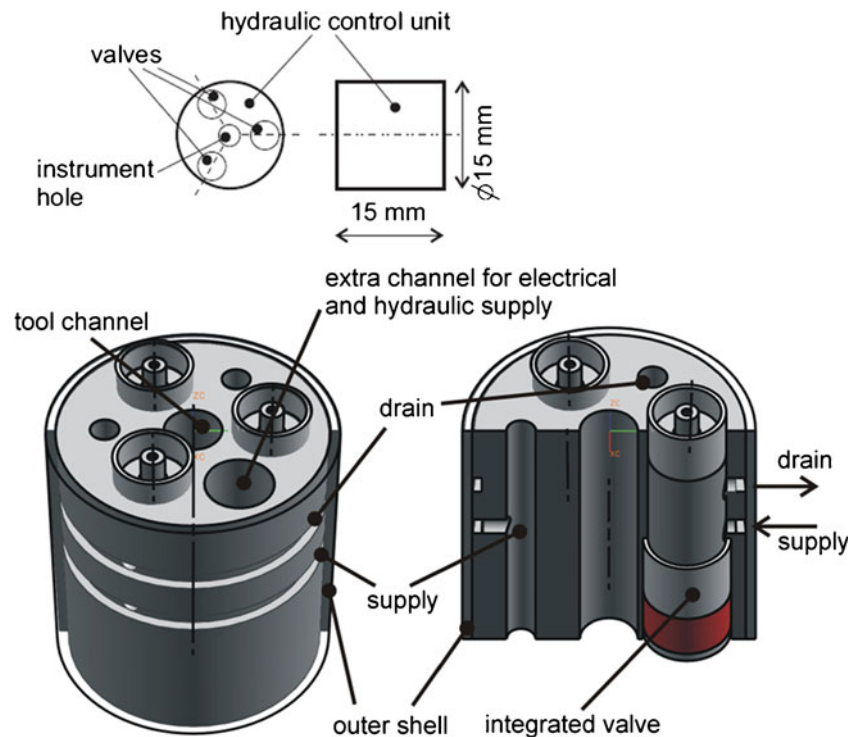
5 Hydraulic control unit

Each flexible segment of the surgical tool has a hydraulic control unit to regulate the pressure that is delivered to each of its McKibben actuators. This hydraulic control unit contains the hydraulic valves for the fluidic actuators, electrical and hydraulic supply channels and fluidic interconnections. Space is also available for electronics and sensors. In the centre of a unit, a hole with a diameter of 3 mm is provided to insert or exchange specific surgical tools during the operation (see tool channel in Fig. 5). An overall diameter of 15 mm was specified as a maximal value for the first prototype as shown in Fig. 5.
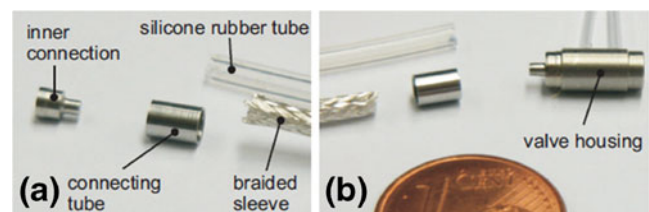
Fig. 4 Images of both extremities of the McKibben actuators during assembly. (**a**) Closed end of the actuator. (**b**) Open end of the actuator direct connected to the supply valve

Fig. 5 (Top) Geometry of the hydraulic control unit. Three valves have to fit inside a housing of 15 mm diameter and 15 mm length. In the centre, a surgical instrument can pass through the tool channel. (Bottom) CAD image of the actual control unit design

As illustrated in Fig. 5, the hydraulic control unit includes three spool valves, one for each McKibben actuator. An extra channel marks the volume that is still available in the control unit and which could be used for electronic control circuitry. At the outside of the housing, grooves are connecting the valves to the drain and to the supply. This part is made out of polycarbonate using precision turning and micromilling. An outer shell of stainless steel closes the grooves (see Fig. 5) and strengthens the housing.

6 Miniaturised hydraulic control valves

To achieve sufficient force density in the braided fluidic actuators a pressure of 8 to 10 bar is required,. When closed, it is preferable that the valve still provides a pressure of 1 bar, which is required to pre-stress the manipulator in the radial direction. This pretension eliminates play between the actuators and the spacer disks. Therefore the valves are designed to control the pressure to the actuators between a range of 1 bar and 8 to 10 bar.

It is important to note that classic membrane type valves developed in silicon technology are not able to cope with the high pressure requirements of this system (Oh and Ahn 2006). Therefore our valve design was inspired on the plunger systems used in large scale hydraulic systems (Urata et al. 1998; Takemura et al. 2008). Our design differs from classic spool valves both because of its size and because it operates with water rather than hydraulic liquid (Doumit et al. 2009).

A schematic representation of the valve is given in Fig. 6 and more details are shown in Figs. 7 and 8. The valve consists of a housing and an axially moving plunger that is actuated by a short stroke (1 mm) linear actuator. The supply and the drain of the valve are incorporated in the valve housing via internal circumferential grooves shown in Fig. 5.

The outlet (1) to the hydraulic actuator is connected with a groove (2) in the plunger (7) of which the position is controlled between the drain (3) and supply (4) to adjust the pressure in the groove and as a result the outlet pressure to the hydraulic actuator. An axial hole (5) and radial hole (6) in the plunger interconnect the groove in the plunger, both ends of the plunger and the outlet to the hydraulic actuator. By connecting both ends of the plunger, the pressure at both sides is equalised. It is important to avoid pressure imbalance as this would result in a disturbance force on the plunger in the axial direction. In the middle position of the plunger, the hydraulic resistances R_3 and R_4 equal $1.5.10^{13}$ N s m^{-5} for a valve with the dimensions discussed below and for water as the hydraulic fluid. It can be noticed that R_i is variable when the plunger is in the most right position. As a result the geometry of the left hydrostatic bearing changes. Experiments showed that this does not compromise the operation of the bearing and the valve.

Fig. 6 Valve Design (a)
Schematic of the spool valve.
(b) Equivalent hydraulic circuit
and its basic representation. The
pressure to the hydraulic
actuator p_{ac} is adjusted by
moving the plunger and thus
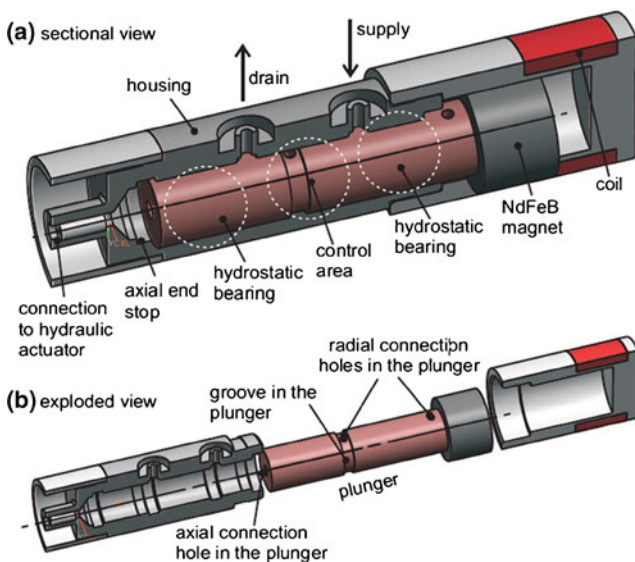changing hydraulic resistances
R_3 and R_4
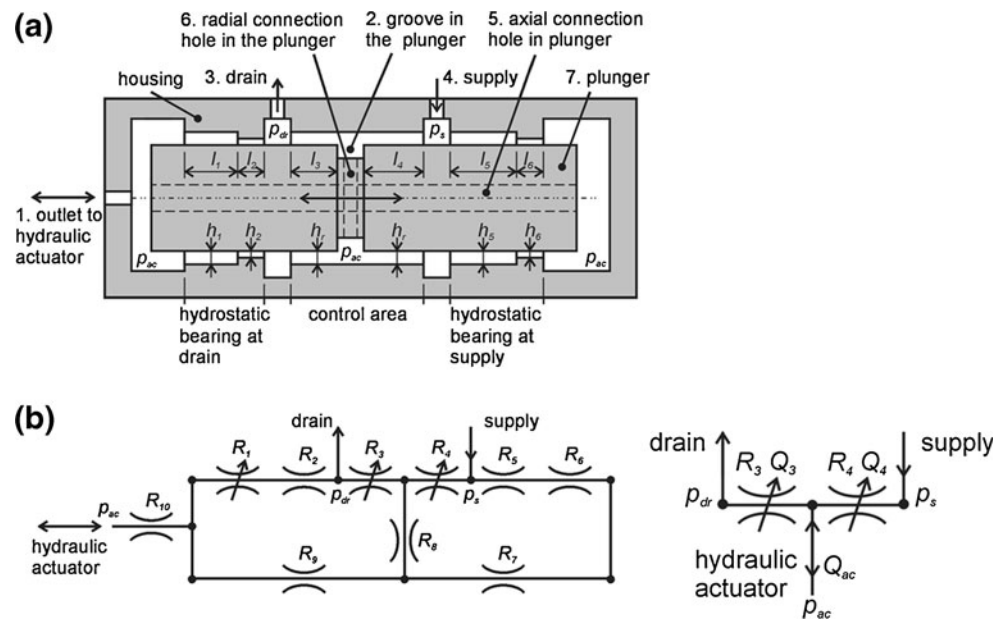
7 Hydrostatic bearings in micro hydraulic systems

A major challenge for the development of precise high
pressure microvalves is to avoid internal friction or
even blockage of the internal parts. Unless preventive
actions are taken, the plunger is pushed against the
housing wall due to any asymmetric pressure distribu-
tion. To avoid stiction problems, and to reduce the
actuation force by minimising friction, miniaturised hy-
drostatic bearings are developed to centre the plunger

Fig. 7 CAD drawing of the valve (a) Section of the spool valve. The
positions of the hydrostatic bearings are indicated by dashed lines. (b)
The exploded view shows the steps for the bearings incorporated in the
housing with an inner diameter of 2 mm

in the housing. Alternative solutions like an elastic
suspension or a membrane cannot align the plunger
within 2 μm to the housing and allow an axial stroke
of 1 mm.

The envisaged valve concept also imposes additional
stringent requirements to the bearing system, as it needs to
keep the plunger with a diameter of 2 mm centred within
2 μm of the housing to guarantee the operation of the valve,
and to avoid collision between moving components. Also,
friction needs to be extremely low in order to enable accu-
rate positioning of the plunger with a small electromagnetic
actuator. This is extremely difficult given the high pressure
load applied to these small valves.

Given the small size of the valve (an outer diameter of
4 mm) and the availability of pressurized fluid, a hydrostatic
bearing has been implemented. In these bearings, the pres-
sure distribution over the circumference of the valve plunger
centres it in the housing. If a disturbance pushes the plunger
away from the centre, a restoring force will drive it back to
the centre as illustrated in Fig. 7. The bearings are supplied
at one side with pressurized fluid, and are connected to the
drain at the other side. From the supply side, the fluid flows
firstly through a gap of 4 μm (2 h) and secondly through a
gap of 2 μm (h) as shown in Fig. 7. Smaller gap sizes would
increase the performance of the bearing and decrease the
leakage, but are not possible due to manufacturing
tolerances.

8 Valve actuator

A small Lorentz actuator with a stroke of 1 mm has been
developed to drive the valve. The Lorentz type actuator
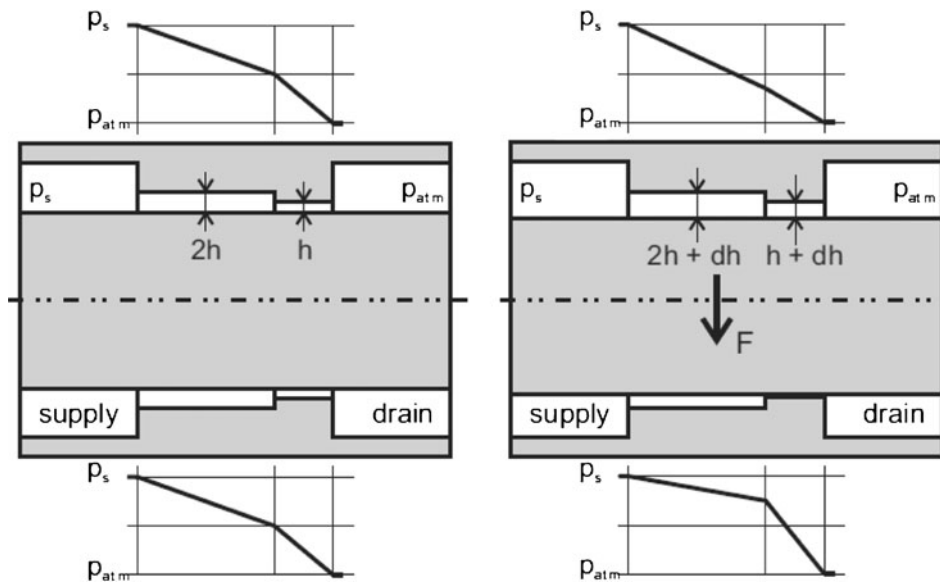
Fig. 8 Working principle of the hydrostatic bearing. If the plunger is centred, the pressure distribution is equal on all sides. A disturbance (indicated by the force F) induces a counteracting pressure distribution as indicated at the right. At the upper part of the valve, the pressure decreases, while the pressure at the lower part increases. The drain pressure is p_{atm} and the supply pressure is p_s

consists of a moving magnet and a fixed coil as shown in Fig. 7. While the NdFeB magnet is attached to the moving plunger and located at the inside of the valve housing, the coil is at the outside of the housing. This configuration assures a leak free valve with no moving wires to a plunger coil.

The output force of the actuator is tested over a range of 2 mm. Because of the varying flux density in the coil volume over the stroke, the output force changes at a constant current. Due to the narrow gap size between the coil housing and the magnet, attention

to the alignment had to be paid to avoid contact. To test the actuator output force, the coil is fixed and the magnet moved within the full stroke with 0.5 mm steps by manually adjusting a set screw. Elastic hinges guide the magnet. At each step, the output force is measured with a force sensor, Tedea type 1,004 600gr. The resolution of the force sensor is 6 mN. Figure 9 shows the actuation force as a function of the magnet position.

The practical implementation of the valve is shown in Fig. 10. The coil has a resistance of $0.85\,\Omega$ and a wire diameter of 0.1 mm. A voltage of 1 V results in a current of 1.2 A and a current density of 127 A/mm^2. The maximal output force is about 45 mN at a relative magnet position of 1.5 mm from the coil. The minimal value is 22 mN at a relative magnet position of 0.5 mm.

Further experiments showed that 1 V was required to achieve sufficient output force to control the plunger position. The heat generated in the coils is removed out of the valve using water that is anyhow present in the valve. Also the small size of the system improves the cooling. The coil is mounted on a paramagnetic aluminium cap sealing the main valve body. So the Lorentz actuator can be considered to be 'ironless'.
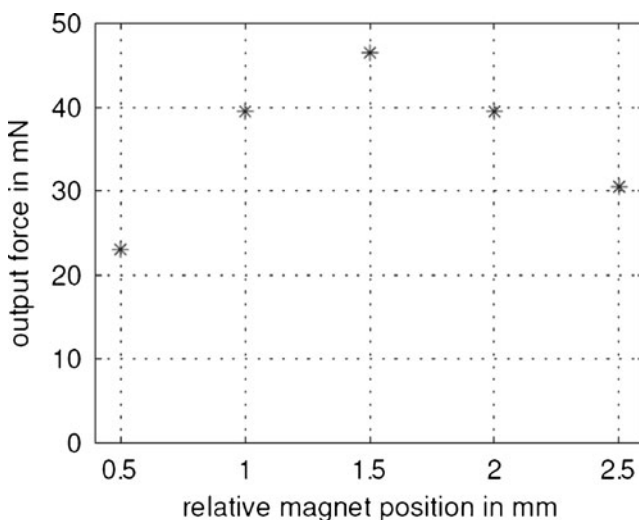

Fig. 9 Experimental results for the actuator output force as a function of the plunger position. The voltage over the coil is kept constant at 1 V, the resistance is $0.85\,\Omega$ and the resulting current is 1.2 A

9 Experimental results microhydraulic valve

To verify the valve behaviour, water at a pressure of 8 bar is supplied to the inlet of a valve. A pressure sensor of the company Druck, type PMP 1,400, measures the controlled outlet pressure. A D-Space system
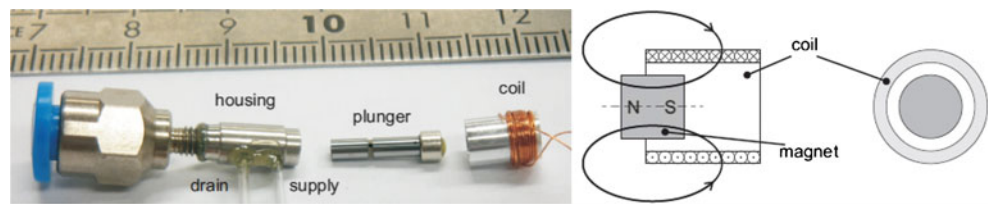
controls the input voltage over the coil as a function of
the measured output pressure. A proportional controller
with an integrator is implemented.

In Fig. 11, the pressure at the outlet of the valve is
plotted for pressure set values between 2 bar and 7 bar
is given. For a supply pressure of 8 bar it was exper-
imentally validated that the outlet pressure can be varied
between 1.5 bar and 6.8 bar. This corresponds to sim-
ulations of the valve behaviour show that the pressure
can be controlled between 1 bar and 7 bar with a
supply pressure of 8 bar.

As shown in Fig. 11, the valve shows good performance
between 2.5 bar and 6 bar. The set value is reached with an
error below 0.1 bar and the rise time (90 % of the set value)
is below 0.1 s. However, the overshoot is 0.3 bar and the
settling time is 1.5 s. For the lowest set value of 2 bar and
the highest set value of 7 bar the deviation between outlet
pressure and set value is more significant. During the
experiments, it was noticed that the valves perform less in
the lower pressure range than at higher values. The imple-
mentation of an integrating action in the valve controller did
not improve the performance. To investigate this behaviour
and to improve the settling time, more insight in the distur-
bance forces on the plunger is required. Also, more ad-
vanced sliding mode controllers have shown to reject

external disturbances in piston cylinder systems (De Volder
et al. 2008), and could therefore help achieving our band-
widths of 10 Hz.

In Fig. 12, experimental results with a triangular input
profile are given. The pressure was varied linearly between
2 bar and 6 bar within 1 s. Since the contraction of the
hydraulic actuators is proportional to the pressure, this
results in a continuous motion of the manipulator. This
graph clearly shows that we can achieve bandwidths of
1 Hz with very small errors.

The experimental results show that the valve meets
the specifications concerning the size and the pressure
range. Three valves fit inside a control unit with a
diameter of 15 mm and a length of 15 mm. The length
of an individual valve is 15 mm including the connec-
tion to the hydraulic actuator. The maximal diameter of
a valve is 4.5 mm.

10 Experimental results of an actuator segment

Information on the actuation properties of individual
McKibben actuators were published in a former paper (De
Volder et al. 2011). Shortly, a McKibben actuator with a
diameter of 1.5 mm was able to achieve a contraction force
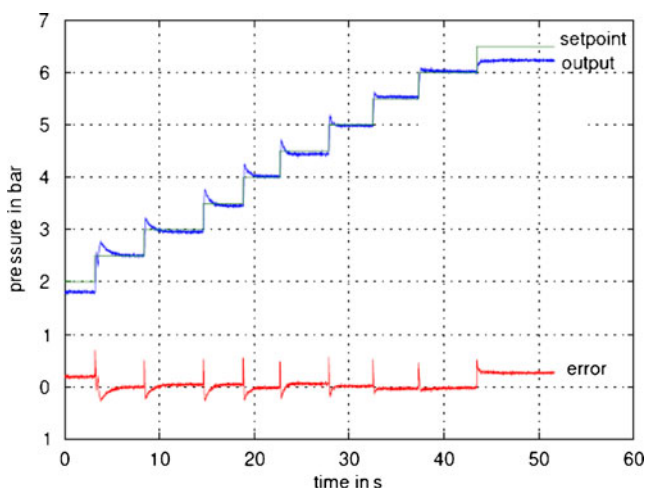
Fig. 11 Pressure control experiments of the valve using a PI controller.
The desired output pressure is changed over time and plotted together
with the error in output pressure
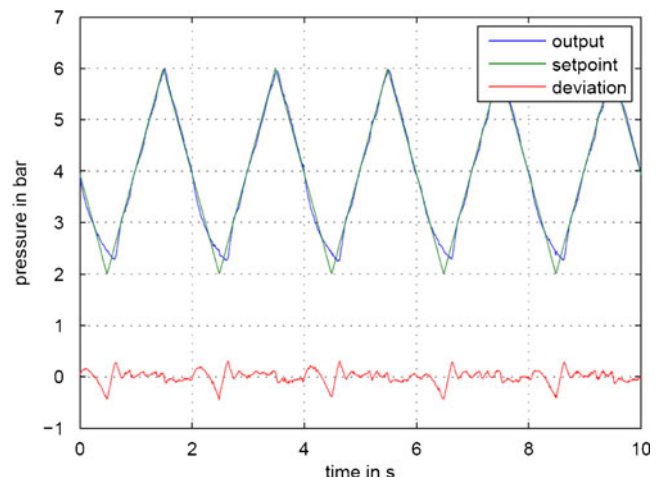
Fig. 12 Response of the valve to a triangular pressure input between
2 bar and 6 bar with a period of 2 s

of 6 N at a supply pressure of 1 MPa, a stroke of about 15 % of the actuator length, and actuation speeds up to 350 mm/s (De Volder et al. 2011). Further feed-back position tests achieved sub-micron positioning accuracy (De Volder et al. 2011).

Examples of surgical manipulators with a gripper tool inserted are shown in Fig. 2, while Fig. 13 shows bending tests on a similar segment. Based on the diameter at which the three fluidic actuator are positioned, the number of spacer disks, the actuator properties and the compliance of the base structure, we estimate that each segment should theoretically be able to achieve bending angles of 150°. Figure 13 shows pictures of the experimental evaluation of a flexible tool segment deflection. The maximal bending angle is 90° in total. We envision that the stroke of this system can still be improved by pre-stretching the actuators in the mount, and by changing the design of the spacer disks which currently restrain the expansion of the actuator. This is the topic of further research.

11 Conclusions

This research introduces a new type of modular surgery tool. It relies on high force hydraulic actuators that can be integrated in a flexible actuator manipulator design. This concept allows the integration of a high number of controlled degrees of freedom inside the patient's body. The main application of this concept is in highly dextrous intra-corporal robotic systems to position instruments deep inside the body and to perform complex surgical tasks. For the control of the fluidic actuators compact high pressure hydraulic valves have been developed. The valves are incorporated with the actuators in a modular system which avoids individual supply tubes to each hydraulic actuator. The valve operation and the motion of a 2-dof motion module have been demonstrated. Importantly, the system can develop high forces needed during the operation, and is at the same time compliant which greatly reduces the requirements on motion accuracy and danger of damaging tissue.
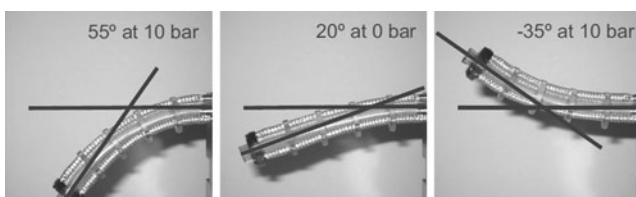
Fig. 13 Experimental evaluation of the segment deflection at different driving pressures

References

G.H. Ballantyne, Robotic surgery, telerobotic surgery, telepresence, and telementoring - Review of early clinical results. Surg. Endosc. **16**(10), 1389–402 (2002)

D.G. Caldwell, G.A. Medranocerda, M.J. Goodwin, Braided pneumatic actuator control of a multi-jointed manipulator, 1993 IEEE International Conference on Systems, Man and Cybernetics, pp. 423–428

A. De Greef, P. Lambert, A. Delchambre, Precis. Eng.-J. Int. Soc. Precis. Eng. Nanotechnol. **33**, 311 (2009)

M. De Volder, D. Reynaerts, Development of a hybrid ferrofluid seal technology for miniature pneumatic and hydraulic actuators. Sens. Actuat. A. Phys. **152**, 234–40 (2009)

M. De Volder, D. Reynaerts, Pneumatic and hydraulic actuators: a review. J. Micromech. Microeng. **20**(4), 043001 (2010)

M. De Volder, J. Coosemans, R. Puers, D. Reynaerts, Characterisation and control of a pneumatic microactuator with an integrated inductive position sensor. Sens. Actuat. A. Phys. **141**, 192–200 (2008)

M. De Volder, F. Ceyssens, D. Reynaerts, R. Puers, J. Microelectro. Syst. **18**, 1100 (2009)

M. De Volder, A. Moers, D. Reynaerts, Fabrication and control of miniature McKibben actuators. Sens. Actuat. A. Phys. **166**(1), 111–6 (2011)

M. Doumit, A. Fahim, M. Munro, Analytical modeling and experimental validation of the braided pneumatic muscle. IEEE Trans. Robot. **25**, 1282–91 (2009)

R. Gaylord, Fluid actuated motor system and stroking device. U. S. Patent **2**, 844–126 (1958)

B. Gorissen, M. De Volder, A. De Greef, D. Reynaerts, Theoretical and experimental analysis of pneumatic balloon microactuators. Sens. Actuat. A. Phys. **168**(1), 58–65 (2011)

K. Harada, D. Oetomo, E. Susilo, A. Menciassi, D. Daney, J.P. Merlet, P. Dario, A reconfigurable modular robotic endoluminal surgical system: vision and preliminary results. Robotica **28**(SI), 171–83 (2010)

S. Hirose, A. Morishima, S. Tukagosi et al. Design of practical snake vehicle: articulated body mobile robot KR-II, 91 ICAR. Fifth International Conference on Advanced Robotics. Robots in Unstructured Environments, Pisa, Italy Date: 19–22 June 1991, vol. 1, pp. 833–838.

O.C. Jeong, S. Konishi, J. Microelectro. Syst. **15**, 896 (2006)

V. Karimyan, M. Sodergren, J. Clark, G.-Z. Yang, A. Darzi, Navigation systems and platforms in natural orifice translumenal endoscopic surgery (notes). Int. J. Surg. **7**, 297304 (2009)

J.-W. Kim, K. Yoshida, K. Kouda, S. Yokota, Sens. Actuat. A. Phys. **156**, 366 (2009)

G. Klute, B. Hannaford, Accounting for elastic energy storage in mckibben articial muscle actuators. Trans. ASME. **122**, 386–8 (2000)

S. Konishi, 2011 International Meeting for Future of Electron Devices (IMFEDK) 2011.

S. Konishi, F. Kawai, P. Cusin, Sens. Actuat. A. Phys. **89**, 28 (2001)

Y.-W. Lu, C.-J. Kim, App. Phys. Let. 89, (2006)

R. Nayyar, N.P. Gupta, Critical appraisal of technical problems with robotic urological surgery. BJU Int. **105**(12), 1710–3 (2010)

K.W. Oh, C.H. Ahn, A review of microvalves. J. Micromech. Microeng. **16**, R13–39 (2006)

J. Peirs, J. Clijnen, D. Reynaerts, H. Van Brussel, P. Herijgers, B. Corteville, S. Boone, A micro optical force sensor for force

feedback during minimally invasive robotic surgery. Sens. Actuat. A. Phys. **115**, 447–55 (2004)

C. Raoufi, A. A. Goldenberg, W. Kucharczyk, J. Biomed. Scie. Engineer. 1, (2008)

D. Reynaerts, J. Peirs, H. Van Brussel, A mechatronic approach to microsystem design. IEEE-ASME Trans. Mech. **3**(1), 24–33 (1998)

A. Ruzzu, K. Bade, J. Fahrenberg, D. Maas, J. Micromech. Microeng. **8**, 161 (1998)

D. Stoianovici, A. Patriciu, D. Petrisor, D. Mazilu, L. Kavoussi, IEEE ASME Trans. Mechatron. **12**, 98 (2007)

K. Suzumori, A. Koga, F. Kondo, R. Haneda, Robotica **14**, 493 (1996)

K. Tadano, K. Kawashima, Adv. Robot. **24**, 1763 (2010)

K. Takemura, S. Park, T. Maeno, J. Sound Vib. **311**, 652 (2008)

E. Urata, S. Miyakawa, C. Yamashina, Y. Nakao, Y. Usami, M. Shinoda, JSME Int. J. Series B. Fluids Therm. Engineer. **41**, 286 (1998)

S. Wakimoto, K. Suzumori, K. Ogura, Adv. Robot. **25**, 1311 (2011)

Y. Watanabe, M. Maeda, N. Yajim, R. Nakamura, H. Iseki, M. Yamato, T. Okano, S. Hori, S. Konishi, Small, soft, and safe microactuator for retinal pigment epithelium transplantation. IEEE MEMS Conf. (2007) pp. 659–62

Y. Watanabe, M. Maeda, N. Yaji, R. Nakamura, H. Iseki, M. Yamato, T. Okano, S. Hori, S. Konishi, 2007 20th IEEE International Conference on Micro Electro Mechanical Systems - MEMS '07 2007.

J.D. Waye, D.K. Rex, C.B. Williams, *Colonoscopy: Principles and Practice*, 2nd edn (Blackwell Publishing Ltd, 2009)

R.J. Webster, A.M. Okamura, N.J. Cowan, Toward active cannulas: miniature snake-like surgical robots, IEEE/RSJ Int. Conf. Intell. Robot. Syst. **1–12**, 2857–63 (2006)

A. Yamaguchi, K. Takemura, S. Yokota, K. Edamura, A robot hand using electro-conjugate fluid. Sens. Actuat. A. Phys. **170**(1–2), 139–46 (2011)